THE EFFECT OF APPLYING MICROBIAL AGENTS ON METABOLITES IN TWO PEANUT FRUITS

LIN, Q. J.[1] – YUE, X. F.[2] – WU, X. X.[1] – GUO, C. J.[1] – ZOU, X.[1] – LI, G.[1] – WANG, J. Z.[1*]

[1]*Institute of Agricultural Quality Standards and Testing Technology, Liaoning Academy of Agricultural Sciences, Shenyang, Liaoning, China*

[2]*Oil Crops Research Institute, Chinese Academy of Agricultural Sciences, Wuhan, Hubei, China*

**Corresponding author*
e-mail: zbswjz72@163.com

(Received 11th May 2024; accepted 25th Sep 2024)

Abstract. This study employed non-targeted metabolomics technology to conduct the research project, identifying a total of 710 cationic metabolites and 426 anionic metabolites across 24 samples. In the Fuhua 36 + compound fertilizer and Fuhua 36 + ARC microbial agents + compound fertilizer, 51 differential metabolites were screened, of which 32 were upregulated and 19 were downregulated. Similarly, the Liaohua 917 + compound fertilizer and Liaohua 917 + ARC microbial agents + compound fertilizer, 70 differential metabolites were identified, with 13 upregulated and 57 downregulated metabolites. 122 differential metabolites were detected in the comparison between Fuhua 36 + compound fertilizer and Liaohua 917 + compound fertilizer, with 58 upregulated and 64 downregulated metabolites. While, 130 differentially expressed metabolites were identified in the comparison of Fuhua 36 + ARC microbial agents + compound fertilizer and Liaohua 917 + ARC microbial agents + compound fertilizer, comprising 94 upregulated and 36 downregulated metabolites, respectively. Utilizing the collected data, we performed comprehensive pathway annotation, differential analysis, and KEGG enrichment analysis for all the identified metabolites. Notably, these metabolites were primarily enriched in the flavonoid biosynthesis pathway. Understanding the metabolic response differences of different peanut varieties to microbial agents can provide reference for breeding peanut varieties with better synergistic effects with microbial agents.
Keyword: *peanut, untargeted metabolomics, ARC-BBBE microbial agent, differential substance screening, KEGG enrichment analysis*

Introduction

Peanut (*Arachis lowgaea* L.) is a significant oil crop renowned for its abundant protein, oil, and nutritional content (Frink et al., 1999). Its protein content, surpassing 30%, ranks second only to that of soybeans. Peanuts are easily absorbed by the human body. The presence of unsaturated fatty acids contributes to cholesterol reduction, while vitamins and minerals promote brain cell development and memory enhancement and exhibit potential anti-tumor, anti-aging, and preventive effects against cardiovascular and cerebrovascular diseases (Camargo et al., 2014). Peanut kernels possess substantial oil content, suitable for extracting high-quality edible oil, and they can be consumed fresh after processing. In 2021, according to data from the National Bureau of Statistics, the peanut cultivation area in China has expanded to 4805 thousand hectares, with Liaoning Province accounting for 323.3 thousand hectares. Remarkably, peanuts have secured the position of being the third largest main crop in the province, after only corn and rice (China Statistical Publishing House, 2022).

There are diverse peanut varieties, and their quality varies widely, lacking a solid scientific foundation for development and utilization. This has significantly

http://www.aloki.hu ● ISSN 1589 1623 (Print) ● ISSN 1785 0037 (Online)
DOI: http://dx.doi.org/10.15666/aeer/2301_061078

inhibited the sustainable progress of the peanut industry. Over the years, substantial efforts have been made to enhance the favorable attributes and characteristics of peanut varieties. Most of these enhancement endeavors have focused on attributes related to growth, drought and disease resistance, along with oil quality and quantity. Only a few studies have been conducted on the enhancement of peanut processing quality (Sithole et al., 2022). The differences in nutritional components and contents across peanut varieties, including metrics such as 100-kernel weight, water content, fat, protein, sucrose, oleic acid, 23.5 kDa and 37.5 kDa subunits of peanut globulin, 18 amino acids, and vitamin E, offer insights into the quality characteristics of both fresh and processed peanut varieties (Zhao et al., 2024) Throughout the ripening process of peanut pods, water content gradually decreases, with large grain kernels possessing a significantly higher water content than medium and small kernels ($P < 0.05$). As the seed kernel matures, there is gradual accumulation of crude protein and crude fat. Notably, the medium-grain type consistently demonstrates higher crude protein content than the small- and large-grain types, while the small-grain type exhibits significantly higher crude fat content than the other varieties ($P < 0.05$). During the podding stage, the soluble sugar and starch content in peanut pods show a declining trend. Remarkably, the starch content of the small-grain type exceeds that of the medium and large-grain types, presenting a significant difference ($P < 0.05$). A correlation analysis of peanut varieties with varying grain types indicates intriguing associations: during pod development, there is a negative correlation between crude fat and crude protein content within the seed kernel, a significant positive correlation between soluble sugar and starch content, and a highly significant negative correlation between crude protein and crude fat content, as well as soluble sugar and starch content (Xie et al., 2021). Reports have indicated that fresh peanuts stored at 4℃ for 120 d using a nitrogen-oxygen mixture (N_2:O_2 = 9:1) and air (control) can exhibit distinctive characteristics. Compared with the control group, the treatment group effectively sustained the freshness of peanuts, increased hardness, retarded the accumulation of malondialdehyde and hydrogen, enhanced antioxidant capacity, and promoted the accumulation of total phenols, flavonoids, and other metabolites (Wu et al., 2022). Under aluminum stress, metabolites within diverse peanut varieties are mainly concentrated in phenolic acids, flavonoids, organic acids, lignans and coumarins, amino acids and their derivatives, and nucleotides and their derivatives (Shen et al., 2022). Notably, no study has examined metabolites within different peanut varieties under conventional fertilization and microbial application.

This study predominantly employed Liquid chromatography tandem mass spectrometry (LC-MS) technology (Dunn et al., 2011; Wilson et al., 2010) combined with multivariate statistical analysis to compare and analyze the chemical composition differences between two primary peanut varieties in Liaoning Province. Leveraging non-targeted metabolomics approaches has proven efficacious in comprehensively analyzing the chemical composition of intricate systems, exploring valuable insights, highlighting significant differences among distinct peanut varieties, and providing a foundational reference for optimizing peanut processing and utilization strategies. Understanding the metabolic response differences of different peanut varieties to microbial agents can provide reference for breeding peanut varieties with better synergistic effects with microbial agents.

http://www.aloki.hu ● ISSN 1589 1623 (Print) ● ISSN 1785 0037 (Online)
DOI: http://dx.doi.org/10.15666/aeer/2301_061078

Materials and methods

Materials

The tested peanut varieties include Fuhua 36 and Liaohua 917, which are high oleic peanut varieties developed by the Peanut Research Institute of Liaoning Academy of Agricultural Sciences.

ARC-BBBE microbial agents sourced from the Oil Crops Research Institute, Chinese Academy of Agricultural Sciences. Microbial agents include: *Bacillus amyloliquefaciens, Bacillus laterosporu* with an effective live bacterial count of ⩾ 200 million/g, and *Bacillus mucilaginosus and Escherichia Ludwiggi* with an effective live bacterial count of ⩾ 1 billion/g.

Peanut compound fertilizer: N-P_2O_5-K_2O = 17-17-17.

Experimental design

Each peanut variety underwent two treatments, CK (without microbial agents) and T (90 kg/hm^2 microbial agents), with each treatment replicated three times. The experiment included two peanut varieties, each covering an area of 100 m^2 and spanning a total of 12 plots. The experimental site was located in Zhangjiakeng Village, Fengjia Town, Zhangwu County, Fuxin City, Liaoning Province, China. Peanut planting commenced on May 10th, where the CK group received conventional peanut compound fertilizer, while the T group was treated with a mixture of ARC-BBBE microbial agents and peanut compound fertilizer for uniform sowing. All other management practices were consistent. Peanut fruits were collected during the harvest period to determine the metabolites in each treatment.

Sample extraction

Sample preparation

After harvesting, peanuts are air dried and sampled. For each treatment, we randomly selected 5 points within the community to extract pods and collected 2 kg of peanuts mixed into one sample. After air drying, the pods are threshed. Divide the obtained sample into 500 g portions using the fractional method and grind the peanut kernels into powder. Dissolve 100 mg of partial powder sample in 1.2 mL of 70% methanol extraction solution. Refrigerate the mixture overnight at 4℃. Subsequently, centrifuge at 12,000 rpm for 10 min, and then extract the supernatant through a 0.22 μ microporous membrane filter. Metabolite analysis of the obtained extract was performed using ultra-high performance liquid chromatography (UPLC) combined with tandem mass spectrometry (MS/MS) (*Table 1*).

Liquid phase conditions

Chromatographic column: Thermo Fisher Hypsil Gold column C18 (100 × 2.1 mm, 1.9 mm μ m).

Mobile phase: A: 0.1% formic acid; B: Methanol; Elution gradient:98% for mobile phase A and 2% for mobile phase B within 0-1.5 min; The ratio of mobile phase A is 15% and mobile phase B is 2% for 1.5-3 min; 3-10 min 100% mobile phase B; 10.1-12 min, mobile phase A ratio is 98%, and mobile phase B ratio is 2%. Flow rate 0.2 mL/min; Column temperature 40°C; The injection volume is 4 μL.

http://www.aloki.hu ● ISSN 1589 1623 (Print) ● ISSN 1785 0037 (Online)
DOI: http://dx.doi.org/10.15666/aeer/2301_061078

Table 1. *Overview of sample conditions*

Sample name	Sample number	Sampling location
Fuhua 36 + compound fertilizer	A1	Zhangwu County, Fuxin City, Liaoning Province
Fuhua 36 + ARC microbial agents + compound fertilizer	B1	
Liaohua 917 + compound fertilizer	A2	
Liaohua 917 + ARC bacterial agents + compound fertilizer	B2	

Mass spectrometry conditions

Scan range selection m/z 100-1500. The settings of ESI source are as follows: spray: 3.5 kV; Sheath gas flow rate: 35 psi; AuxGas flow rate:10 L/min; Capillary Temperature: 320℃; S-lens RF level: 60; Aux gas heater temperature: 350℃; Polarity: positive, negative; MS/MS secondary scans are data dependent scans

Data processing and statistical analysis

The raw data were preprocessed using CD3.1 data processing software. The molecular weight of each metabolite was determined on the basis of the mass-to-charge ratio (m/z) of the parent ions in the primary mass spectrometer. Subsequently, the molecular formula was predicted using parameters such as mass number deviation (ppm) and adduct ions, followed by database matching. The database containing secondary spectra was utilized to match actual secondary spectra with data such as fragment ions and collision energies for each metabolite in the database. This process makes secondary identification of metabolites possible. Metabolites displaying Coefficients of Variation (CV) below 30% (Wei et al., 2017) in QC samples were retained as the final identification results for subsequent analyses.

Results

Total sample analysis

A total of 710 metabolites were identified across all samples and categorized into 10 distinct types of metabolites. These categories included lipids and lipid-like molecules (25.51%), phenylpropanoids and polyketides (17.49%), organic acids and derivatives (16.05%), organic heterocyclic compounds (12.96%), benzenoids (10.08%), organic oxygen compounds (6.17%), nucleosides, nucleotides, and analogs (3.70%), lignin, neosignals, and related compounds (2.88%), alkaloids and derivatives (1.65%), organic nitrogen compounds (1.44%), homogeneous non-metallic compounds (0.21%), and hydrocarbons (0.21%), as illustrated in *Figure 1*.

Principal component analysis

Principal component analysis (PCA) was conducted on the samples, including quality control (QC), to gain a preliminary understanding of the overall metabolic differences among the four sample groups and the magnitude of variability between samples within the group (Wen et al., 2017). As depicted in *Figure 2*, the raw data obtained from LC-MS exhibited distinct separation along the principal components PC1 and PC2. The contribution rates of the first and second principal components were 21.78% and 14.68% for A1vsA2 (Fuhua 36 + compound fertilizer, Liaohua 917 + compound fertilizer),

http://www.aloki.hu ● ISSN 1589 1623 (Print) ● ISSN 1785 0037 (Online)
DOI: http://dx.doi.org/10.15666/aeer/2301_061078

respectively, with the sum of the contribution rates being 36.46%. For A1vsB1 (Fuhua 36 + compound fertilizer, Fuhua 36 + ARC microbial agents + compound fertilizer), the contribution rates of the first and second principal components were respectively 18.78% and 16.58%, with the sum of contribution rate being 35.36%. For B1vsB2 (Fuhua 36 + ARC microbial agents + compound fertilizer, Liaohua 917 + ARC microbial agents + compound fertilizer), the contribution rates of the first and second principal components were 30.70% and 17.16%, respectively, with the sum of the contribution rates being 47.86%. Similarly, for A2vsB2 (Liaohua 917 + compound fertilizer, Liaohua 917 + ARC microbial agents + compound fertilizer), the contribution rates of the first and second principal components were 29.56% and 15.79%, respectively, with the sum of the contribution rates being 45.35%. The PCA distinctly separated Fuhua 36 and Liaohua 917. Cluster heat map analysis of the four sample groups (Chen et al., 2015) (*Fig. 3*) demonstrated noticeable differences among the groups, and parallel samples within each group exhibited resemblances, providing sample reliability.

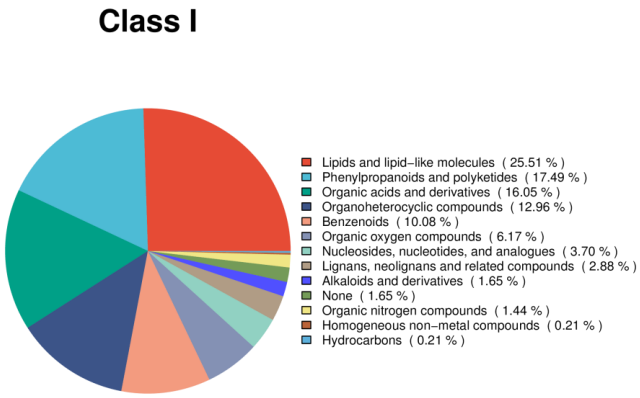

Figure 1. *Metabolite classification*

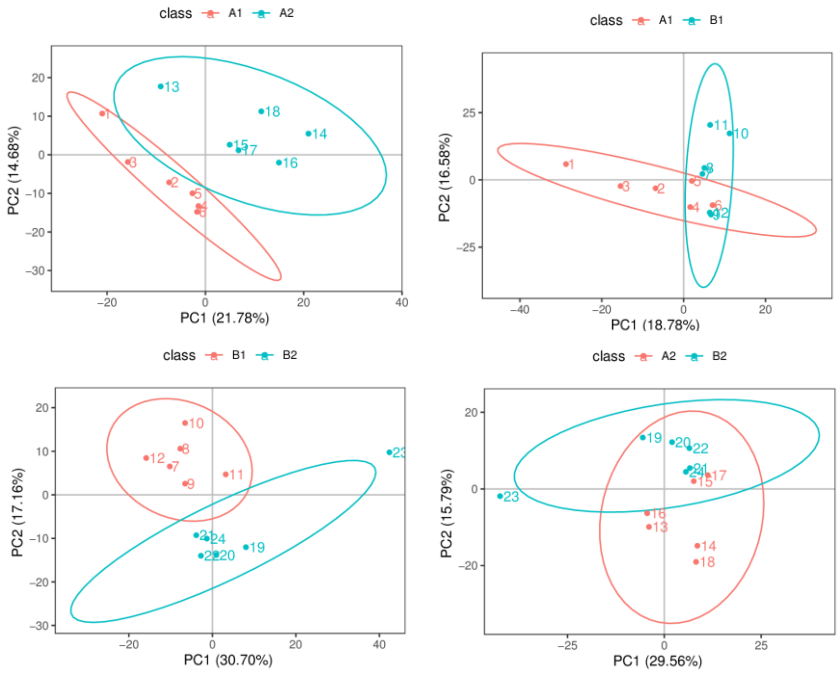

Figure 2. *PCA score*

http://www.aloki.hu ● ISSN 1589 1623 (Print) ● ISSN 1785 0037 (Online)
DOI: http://dx.doi.org/10.15666/aeer/2301_061078

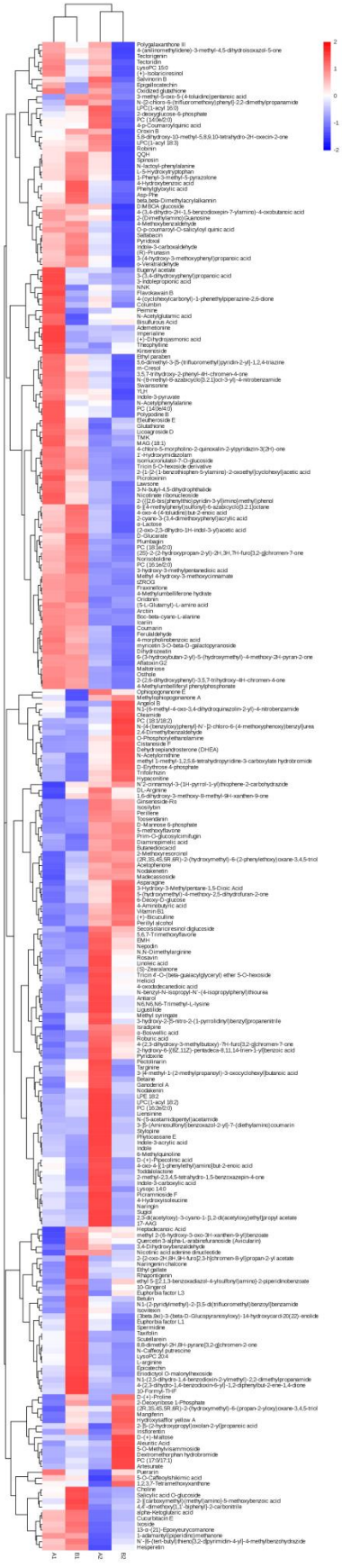

Figure 3. *Cluster heat map analysis of the four sample groups*

APPLIED ECOLOGY AND ENVIRONMENTAL RESEARCH 23(1):61-78.
http://www.aloki.hu ● ISSN 1589 1623 (Print) ● ISSN 1785 0037 (Online)
DOI: http://dx.doi.org/10.15666/aeer/2301_061078

Partial least squares discriminant analysis

The metabolomic data were subjected to analysis using the Partial Least Squares Discriminant Analysis (PLS-DA) model (Boulesteix et al., 2007; Wang et al., 2014), with the following model parameters: A1vsB1 R2Y = 0.98 and Q2Y = 0.32; B2vsA2 R2Y = 0.89, Q2Y = 0.45; A1vsA2 R2Y = 1, Q2Y = 0.69; and B1vsB2 R2Y = 0.97 and Q2Y = 0.73. R2Y represents the explanatory power of the model, while Q2Y assesses the predictive performance of the PLS-DA model. When R2Y surpasses Q2Y, it indicates a robust model with reliable predictive capability.

Screening and analysis of differential metabolites

Based on PLS-DA analysis, the threshold values were set to VIP > 1.0, FC > 1.2, or FC < 0.833 with P-value < 0.05 (Boulesteix et al., 2007; Wang et al., 2014) for the differential metabolite screening process. The results of the screening are presented in *Table 2*. Distinct differences were observed among the 710 metabolites detected. In the case of B1vsA1, 51 differential metabolites were screened, including 32 upregulated and 19 downregulated metabolites (*Fig. 4A*). Furthermore, for B2vsA2, 70 differential metabolites were screened, of which 13 were upregulated and 57 were downregulated (*Fig. 4B*). 122 differential metabolites were screened from A1vsA2, among which 58 were upregulated and 64 were downregulated (*Fig. 4C*). Additionally, 130 differentially expressed metabolites were screened in B1vsB2, with 94 upregulated and 36 downregulated metabolites (*Fig. 4D*).

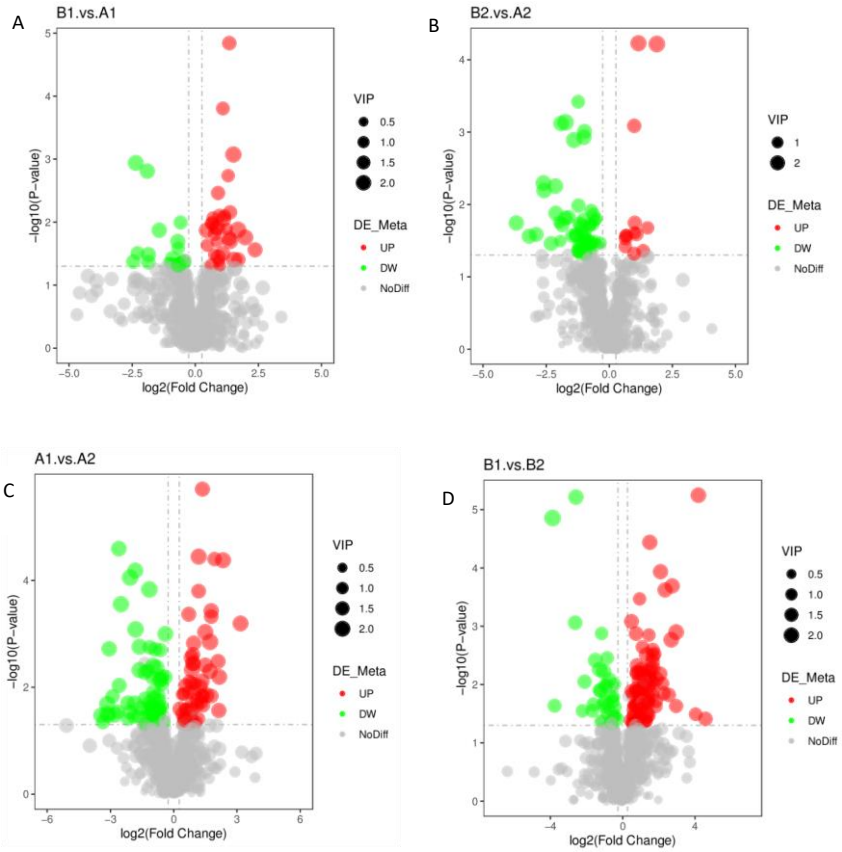

Figure 4*. Volcano Plot of Differential Metabolites Between Groups*

Figure 4. *Volcano plot of differential metabolites between groups*

http://www.aloki.hu ● ISSN 1589 1623 (Print) ● ISSN 1785 0037 (Online)
DOI: http://dx.doi.org/10.15666/aeer/2301_061078

Table 2. *Results of metabolite difference screening*

Compared samples	Num. of total ident.	Num. of total sig.	Num. of sig. up	Num. of sig. down
B1.vs.A1_pos	710	51	32	19
B2.vs.A2_pos	710	70	13	57
A1.vs.A2_pos	710	122	58	64
B1.vs.B2_pos	710	130	94	36

Upon applying log2FC treatment to the detected metabolites, we identified the top 20 differential metabolites that exhibited the most significant changes in both the upregulated and downregulated directions.

When applying compound fertilizer without adding ARC-BBBE microbial agent, a significant increase in the relative content of 3-hydroxy-3-methylpentanoic acid, tryptophan 5-hexoside derivatives, adenosylmethionine, 3-(3,4-dihydroxyphenyl) propionic acid, icariin, 2-(2,6-dihydroxyphenyl)-3,5,7-trihydroxy-4H-chromo-4-one, cenone, tZROG, baihuadansu, and 1-adamantine (piperidyl) ketone was observed in A1vsA2. Conversely, a notable decrease in the relative contents of PC (16:2e/2:0), mannitol A, LPC (1-acyl 18:2), lotus seed alkaloid, LPE (18:2), α-boswellic acid, dehydroepiandrosterone (DHEA), N-benzyl-N-isopropyl-N'-(4-isopropylphenyl) thiourea, ginsenoside Ro, and 3-[5-(aminosulfonyl) benzoxazol-2-yl]-7-(diethylamino) coumarin was observed (*Fig. 5*).

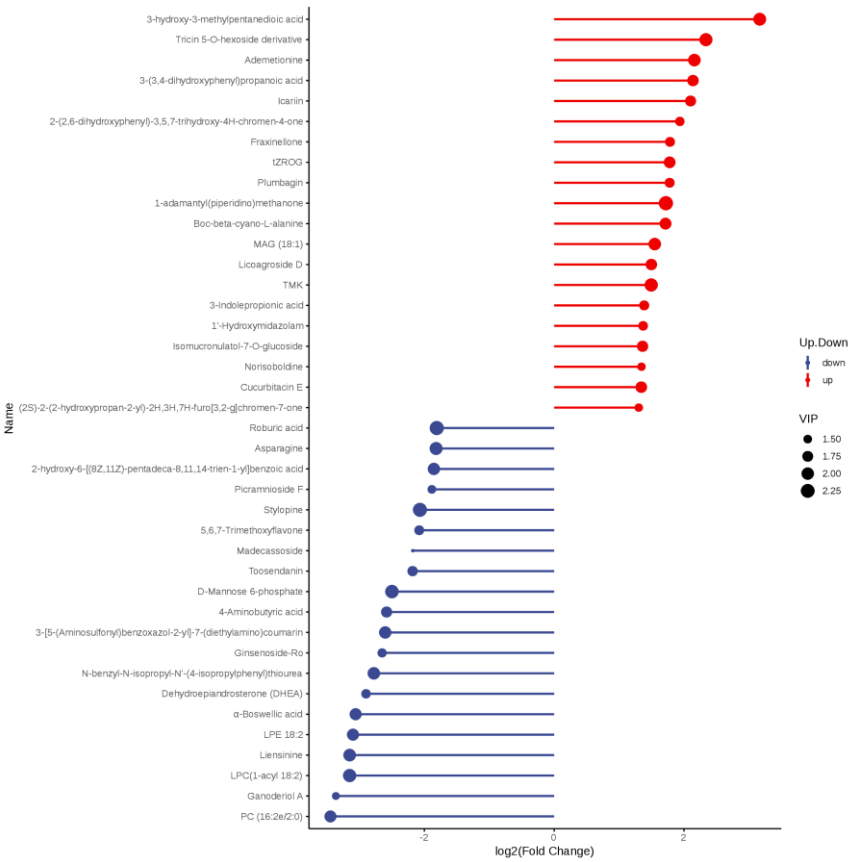

Figure 5. *20 Bubble plot displaying the top 20 metabolites with the highest content differences in A1vsA2 samples*

http://www.aloki.hu ● ISSN 1589 1623 (Print) ● ISSN 1785 0037 (Online)
DOI: http://dx.doi.org/10.15666/aeer/2301_061078

In the B1vsA1, there were substantial increases in several characteristics such as the relative contents of 10-gingerol and quercetin-3-α-L-arabinofuranoside (amygdalin), Euphorbia factor L3, 2-{2-oxo-2H, 8H, 9H furano [2,3-h] chromoen-8-yl} propyl-2-yl acetate, Salvia emodin, 5-[(2,1,3-benzoxadiazol-4-ylsulfonyl) amino]-2-piperidinylbenzoate ethyl ester, mangiferin, heptadecanoic acid, N1-(2-pyridyl)-2-[3,5-bis(trifluoromethyl)benzoyl] benzamide, and isovitexin. The relative contents of NNK, adenosylmethionine, sibirin, red clover root glucoside, N-acetylglutamate, fritillarin A, 4-(cyclohexylcarbonyl)-1-phenylethylpiperazin-2,6-dione, picroside F, D-(+) pipecolic acid, and pyrosulfite significantly decreased (*Fig. 6*).

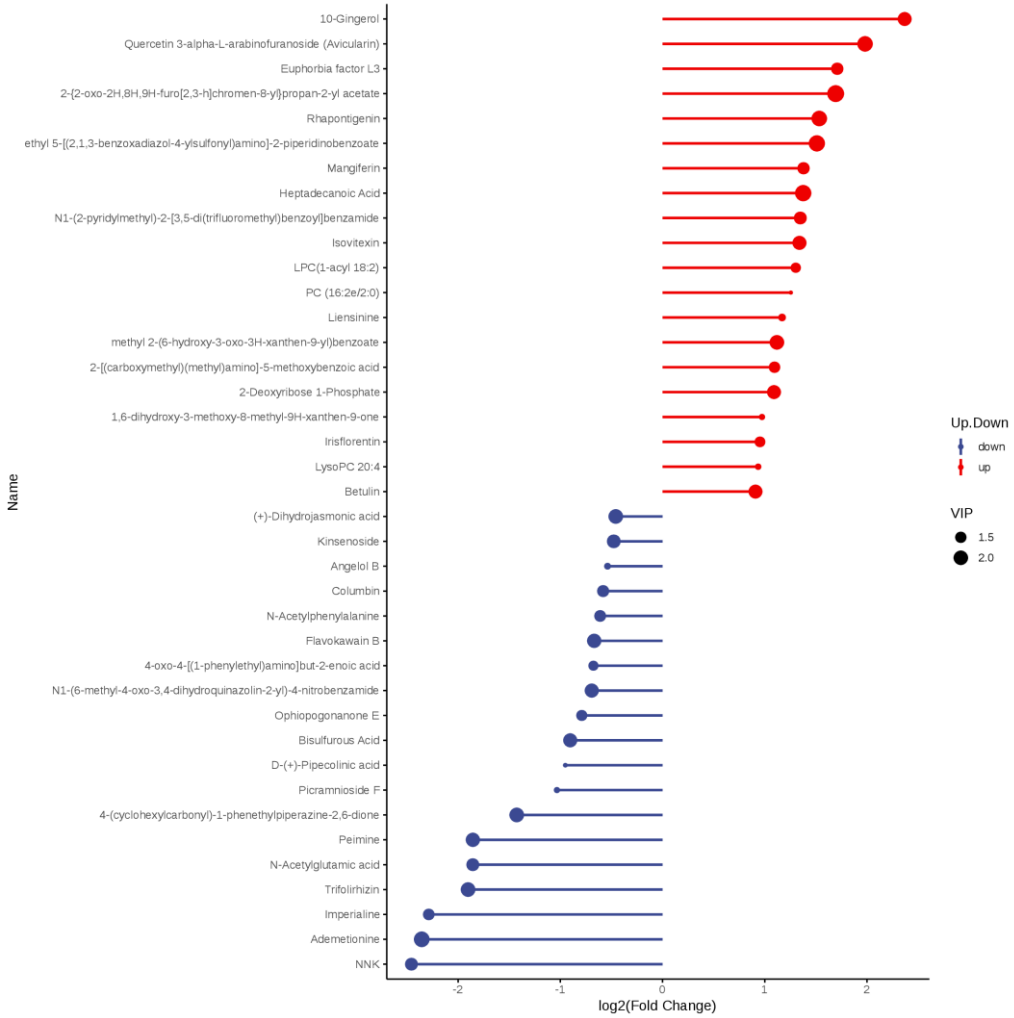

Figure 6. *Bubble plots visualizing the top 20 metabolites with the highest content differences in B1vsA1 samples*

In B2vsA2 both inoculated and non-inoculated, the significantly increased relative contents were detected in PC (17:0/17:1), 5-O-caffeoyl shikimic acid, 1,2,3,7-tetramethoxyflavone, 2-[5-(2-hydroxypropyl)oxoan-2-yl] propionic acid, shellac acid, 5-O-methylvisaminide, 1-adamantinyl (piperidyl) ketone, artesunate, D-(+) maltose, and oleamide. The relative contents of PC (16:2e/2:0), liensinine, LPC (1-acyl18:2), 3-5-(aminosulfonyl) benzoxazol-2-yl-7-(diethylamino) coumarin, picroside F, 17-AAG, 4-

http://www.aloki.hu ● ISSN 1589 1623 (Print) ● ISSN 1785 0037 (Online)
DOI: http://dx.doi.org/10.15666/aeer/2301_061078

hydroxyisoleucine, D (+) piperidine, 6-[(4-methylphenyl) sulfonyl]-6-azabicyclic [3.2.1] octane, N1- 2,3-dihydro-1,4-benzodioxane-2-ylmethyl)-2,2-dimethylpropanamide were significantly decreased (*Fig. 7*).

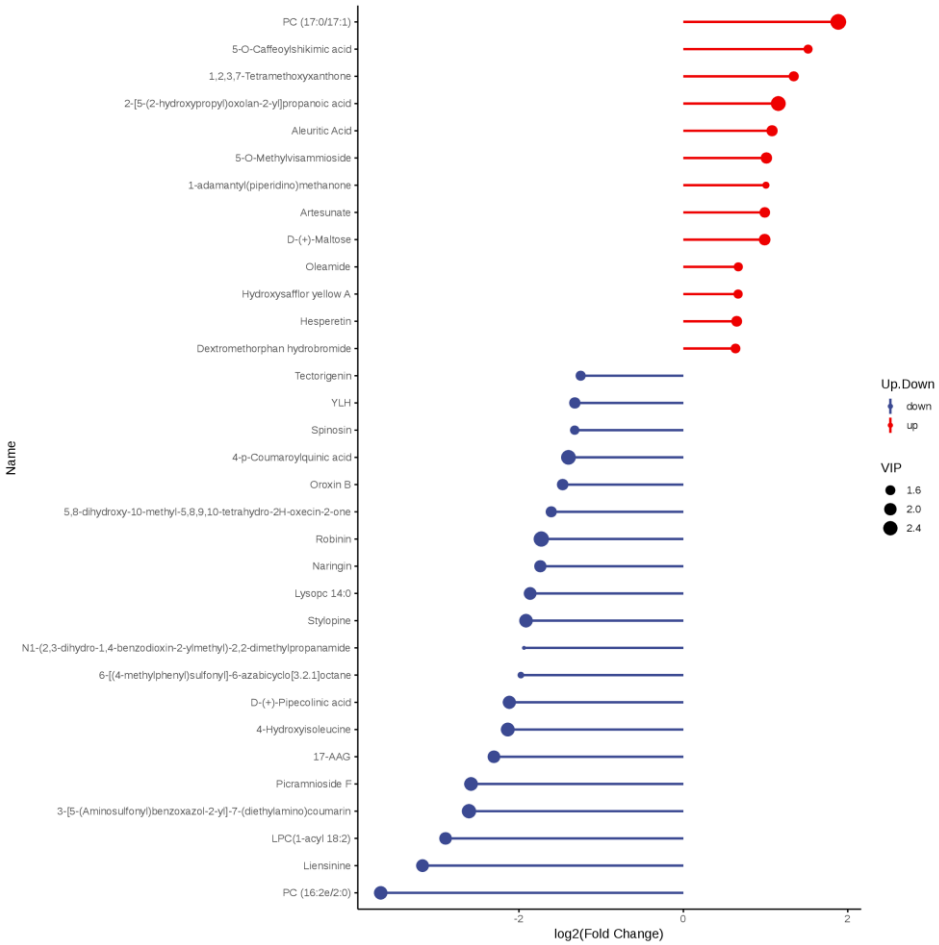

Figure 7. *Bubble plots depicting the top 20 metabolites with the highest content differences in B2vsA2 samples*

In B1vsB2, significant increases were observed in certain relative contents such as N1-(2,3-dihydro-1,4-benzodioxane 2-ylmethyl)-2,2-dimethylpropionamide, 3-hydroxy-3-methylpentanoic acid, 4-(2,3-dihydro-1,4-benzodioxane), baihuadansu, 8,8-dimethyl-2H, 8H-pyran(3,2-g)chromo-2-one, tryptophan 5-hexoside derivative, 2-(2,6-dihydrophenyl)-3,5,7-trihydroxy-4H-chromo-4-one, scutellarin, and tZ. ROG. The relative contents of red clover root glycoside, dehydroepiandrosterone (DHEA), 4-aminobutyric acid, 6-phosphate D-mannose, ginsenoside Ro, PC (18:1/18:2), α-boswellic acid, toosendanin, diaminoheptanedioic acid, and succinic acid were significantly decreased (*Fig. 8*).

KEGG enrichment analysis

Using KEGG analysis (Kanehisa, 2000; Rao et al., 2014; Lin et al., 2014; Zhang et al., 2016), a total of 36 metabolic pathways exhibited changes in A1vsA2. From these pathways, the top 20 were selected based on the P-value ranking from small to large and

http://www.aloki.hu ● ISSN 1589 1623 (Print) ● ISSN 1785 0037 (Online)
DOI: http://dx.doi.org/10.15666/aeer/2301_061078

are represented in a bubble diagram (*Fig. 9*). Notably, the enrichment of several significant pathways was confirmed by combining P-values, including butanoate metabolism, citrate cycle (TCA cycle), pentose and glucuronic acid interconversion, fructose and mannose metabolism, benzoxazinid biosynthesis, linoleic acid metabolism, and alanine pathways (*Fig. 9*). In particular, the alanine, aspartate, and glutamate metabolic pathways were notably enriched. In the butyric acid metabolism pathway, there was a notable downregulation of L-glutamate and 4-aminobutyric acid expression. The expression of 2-oxoglutarate was upregulated in the tricarboxylic acid cycle. Downregulation was evident in the expression of D-mannose-6p within the fructose and mannose metabolic pathways as well as in the expression of indole within benzoxazine biosynthesis-related pathways. Similarly, the expression of linoleic acid in the linoleic acid metabolic pathway was downregulated. In the context of metabolic pathways, alanine, aspartic acid, glutamate, adenylate succinate, L-arginine succinate, and 4-aminobutyric acid (GABA) were downregulated, whereas glutamate and 2-oxoglutarate were upregulated.

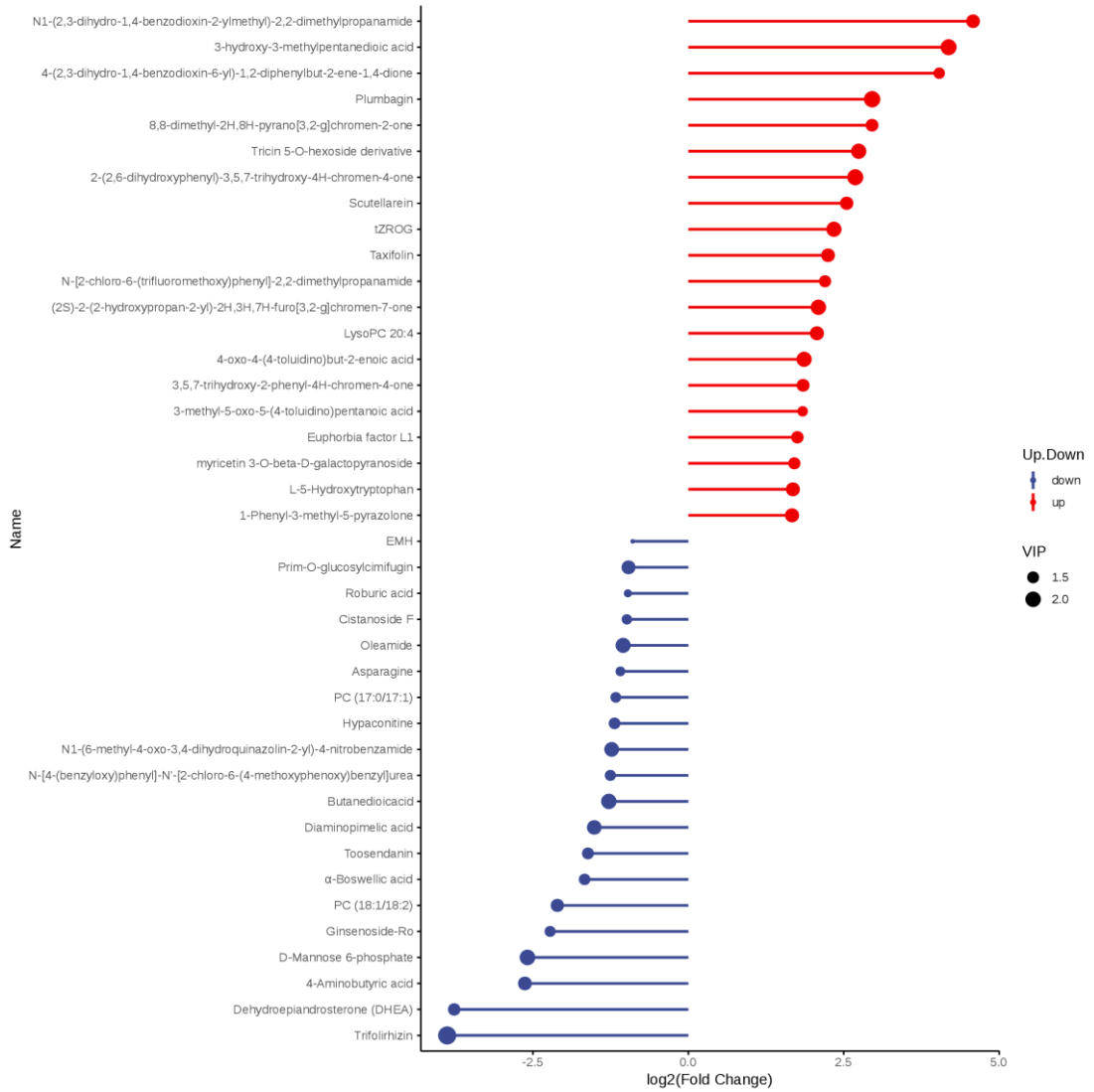

Figure 8. *Bubble plots showing the top 20 metabolites with the highest content differences in B1vsB2 samples*

http://www.aloki.hu ● ISSN 1589 1623 (Print) ● ISSN 1785 0037 (Online)
DOI: http://dx.doi.org/10.15666/aeer/2301_061078

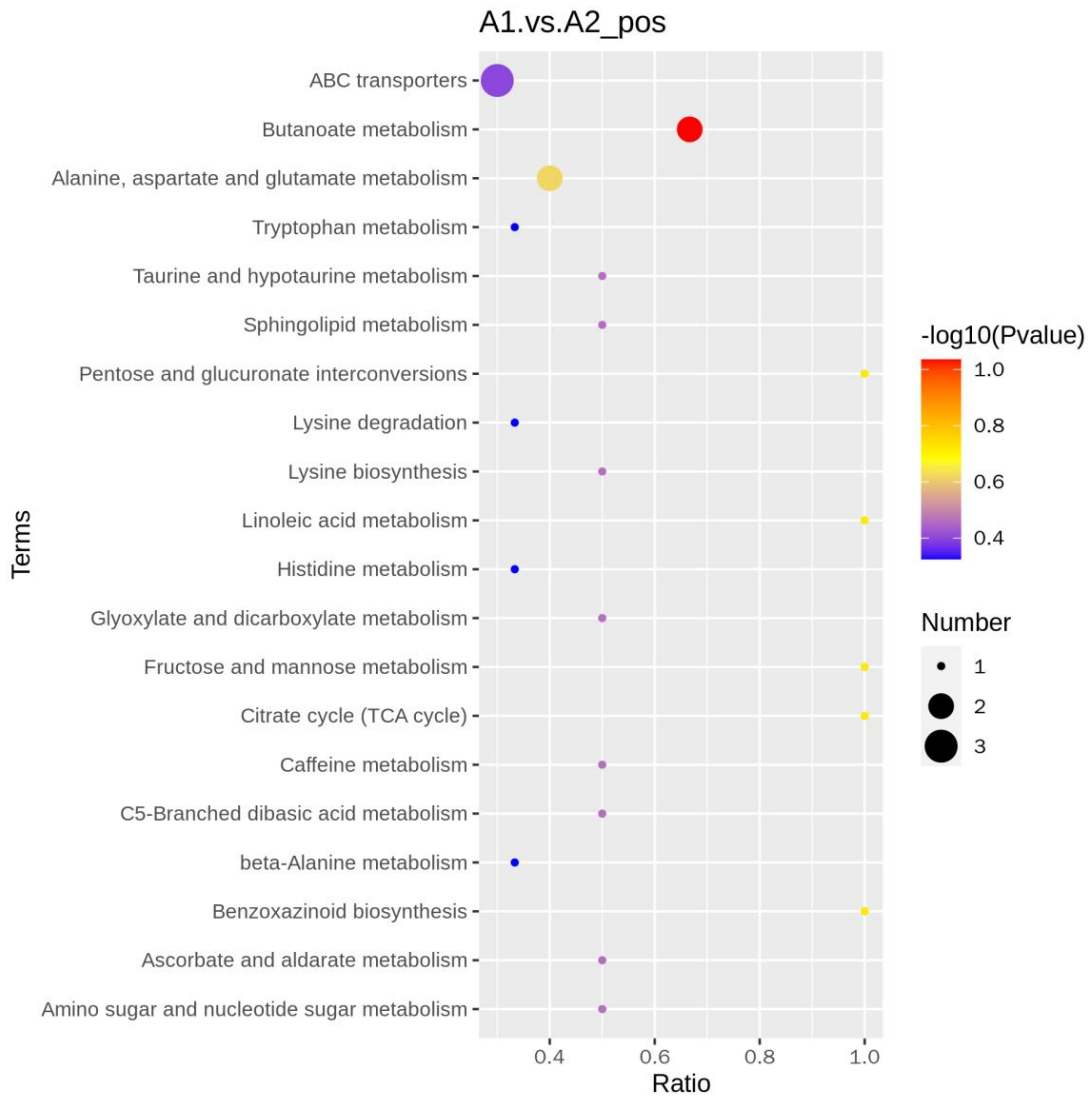

Figure 9. *Metabolic enrichment bubble chart for A1 and A2 samples*

The results regarding metabolite differences between B2vsA2 indicated changes in 12 metabolic pathways (*Fig. 10*). Notably, the pathways for flavonoid biosynthesis, benzoxazine biosynthesis, phenylpropanoid biosynthesis, lysine degradation, tryptophan metabolism, vitamin B6 metabolism, and phenylalanine metabolism were substantially enriched. In flavonoid biosynthesis, naringin was downregulated, whereas hesperidin and caffeic acid were upregulated. Indole was downregulated in the biosynthetic pathway of benzoxazine. In the phenylpropanoid biosynthesis pathway, coumarin was downregulated, and 5-O-caffeoyl shikimic acid was upregulated. Furthermore, the lysine degradation pathway indicated the downregulation of trimethyllysine expression. In the tryptophan metabolism pathway, indole expression was downregulated, and pyridoxine expression was downregulated in the vitamin B6 metabolic pathway.

In the context of B1vsA1, significant alterations spanning 12 metabolic pathways were observed compared with the non-bacterial agent condition (*Fig. 11*). Among these pathways, high enrichment was observed in the one-carbon pool of folate, one-carbon

http://www.aloki.hu ● ISSN 1589 1623 (Print) ● ISSN 1785 0037 (Online)
DOI: http://dx.doi.org/10.15666/aeer/2301_061078

pool by folate, flavonoid biosynthesis, flavonoid and flavonol biosynthesis, carbon metabolism, β-alanine metabolism, and alanine metabolism. Notable results included the upregulation of 10-formyl-THF expression in the carbon pool metabolic pathway of folic acid, downregulation of red clover root glycoside expression in the flavonoid biosynthesis pathway, upregulation of isovitexin expression in the biosynthesis pathway of flavonoids and flavonols, and upregulation of 10-formyl-THF expression in the carbon metabolism pathway. The β-alanine metabolism pathway upregulated spermidine expression.

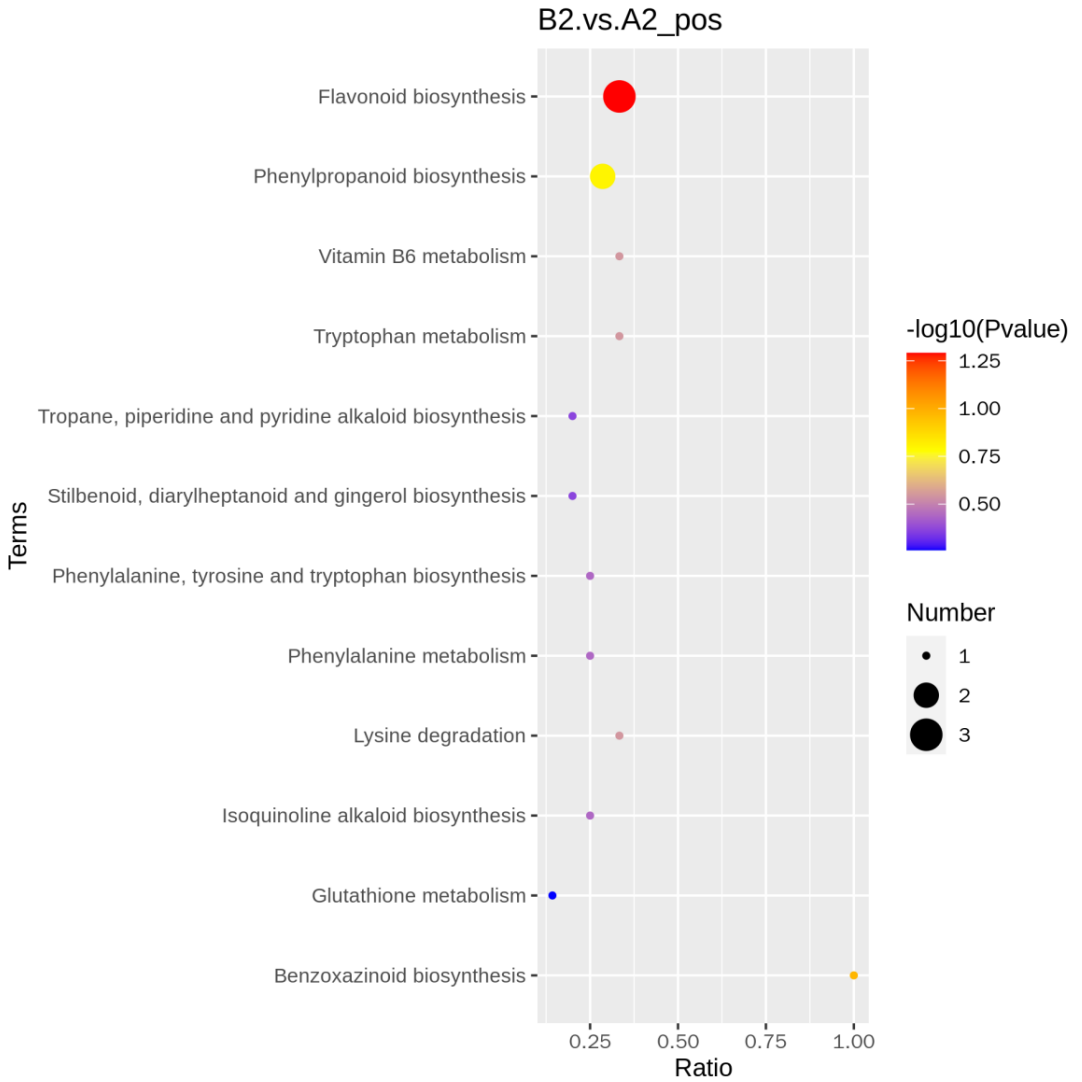

Figure 10. *Metabolic enrichment bubble chart for B2 and A2 samples*

The metabolic differences between B1vsB2, indicated changes in 29 metabolic pathways. The top 20 pathways, determined based on small-to-large P-value rankings, were selected for visualization in a bubble chart (*Fig. 12*). Significant metabolic pathways emerged, including carbon metabolism, β-alanine metabolism, vitamin B6 metabolism, phenylpropanoid biosynthesis, arginine and proline metabolism, phenylalanine metabolism, pentose phosphate pathway, fructose and mannose

http://www.aloki.hu ● ISSN 1589 1623 (Print) ● ISSN 1785 0037 (Online)
DOI: http://dx.doi.org/10.15666/aeer/2301_061078

metabolism, one-carbon pool of folate, carbon fixation in photosynthetic organisms, monoterpene biosynthesis, flavonoid biosynthesis, and prominently enriched ABC transporters. In the carbon metabolism pathway, 10-formyl-THF was upregulated, whereas D-erythritol was downregulated. The expression of spermidine in the β-alanine metabolism pathway was upregulated, pyridoxine expression was upregulated in the vitamin B6 metabolism pathway, and D-erythritol and 4-phosphate were downregulated. The phenylpropanoid biosynthesis pathway upregulated the expression of spermidine and coumarin. D-erythritol was downregulated in the pentose phosphate pathway. Downregulation of mannose expression was observed in the fructose and mannose metabolic pathways. Moreover, 10-formyl-THF expression in the one-carbon pool of folate pathway is upregulated. Notably, the carbon fixation effect within the photosynthetic pathway indicated downregulated erythritol expression. The monoterpene biosynthesis pathway reflected downregulated perilla alcohol expression, whereas the flavonoid biosynthesis pathway showed downregulated purslane-3-O-glucoside expression. Distinct upregulation of vitamin B1, spermidine, maltotriose, and choline was evident among ABC transporters.

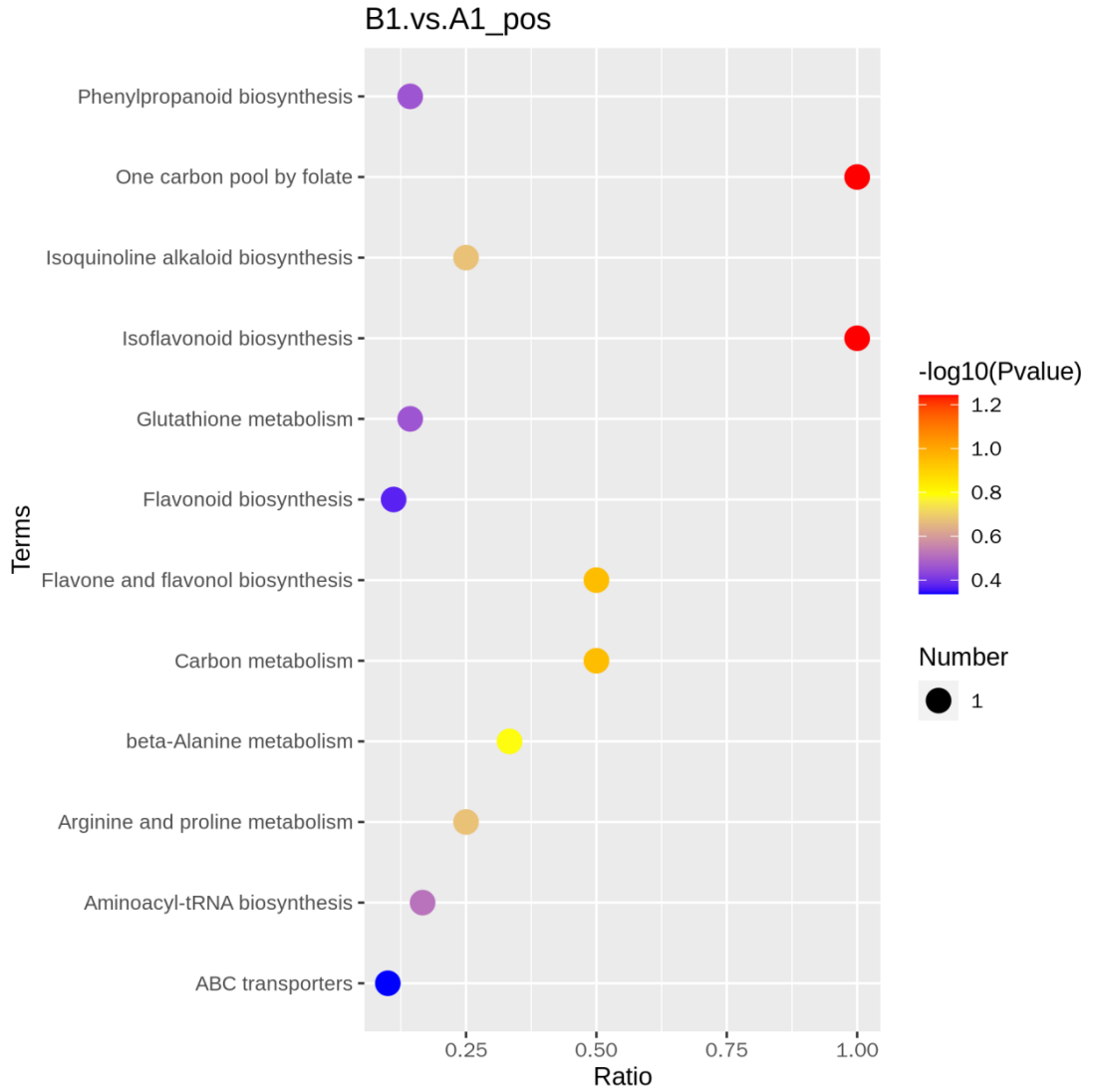

Figure 11. *Metabolic enrichment bubble chart for B1 and A1 samples*

http://www.aloki.hu ● ISSN 1589 1623 (Print) ● ISSN 1785 0037 (Online)
DOI: http://dx.doi.org/10.15666/aeer/2301_061078

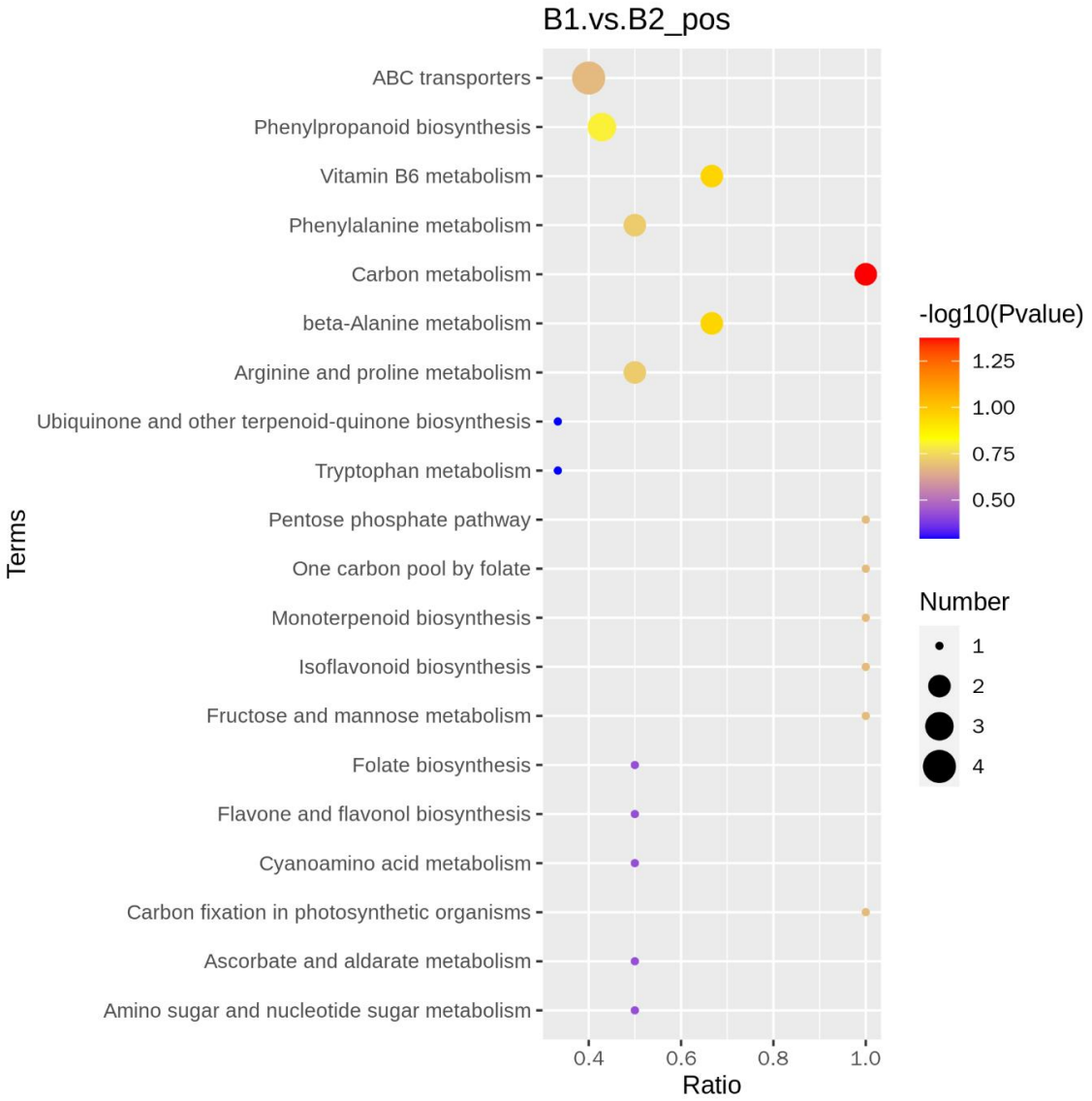

Figure 12. *Metabolic enrichment bubble chart for B1 and B2 samples*

Conclusion

Metabolomics, an interdisciplinary field, requires the comprehensive application of diverse disciplines to provide comprehensive and accurate insights into substance information. A comprehensive and detailed understanding of metabolic abnormalities and differences is a pivotal characteristic of metabolomics. This study employed UPLC-HRMS non-targeted metabolomics to analyze metabolite profiles in application of microbial agents to two peanut varieties. Among the 710 detected metabolites, B1vsA1 comparison presented 51 differential metabolites, including 32 upregulated and 19 downregulated metabolites. Similarly, the B2vsA2 comparison identified 70 differential metabolites, with 13 upregulated and 57 downregulated metabolites. In the A1vsA2 comparison demonstrated 122 differential metabolites, with 58 upregulated and 64 downregulated metabolites. Concurrently, in the B1vsB2 comparison yielded 130 differentially expressed metabolites, with 94 upregulated and 36 downregulated metabolites.

http://www.aloki.hu ● ISSN 1589 1623 (Print) ● ISSN 1785 0037 (Online)
DOI: http://dx.doi.org/10.15666/aeer/2301_061078

Effects of different peanut varieties on root metabolism

Under conventional application of compound fertilizer without adding ARC BBBE microbial agent, the expression of 4-aminobutyric acid in the butyric acid metabolism pathways of Fuhua 36 and Liaohua 917 was downregulated. Mannose was downregulated in the fructose and mannose metabolism pathway, and indole was downregulated in the phenylpropanediamine metabolism pathway. The relative contents of 3-hydroxy-3-methylpentanoic acid, tryptophan 5-hexoside derivatives, adenosylmethionine, 3-(3,4-dihydroxyphenyl) propionic acid, icariin, 2-(2,6-dihydroxyphenyl)-3,5,7-trihydroxy-4H-chromo-4-one, cenone, tZROG, baihuadansu, and 1-adamantine (piperidyl) ketone significantly increased. The relative contents of PC (16:2e/2:0), mannitol A, LPC (1-acyl 18:2), liensinine, LPE (18:2), α-boswellic acid, dehydroepiandrosterone (DHEA), N-benzyl-N-isopropyl-N'-(4-isopropylphenyl) thiourea, ginsenoside Ro, 3-[5-(aminosulfonyl) benzoxazol-2-yl]-7-(diethylamino) coumarin was significantly reduced.

Metabolic effects of microbial agents on the root systems of different peanut varieties

Under the conditions of conventional application of compound fertilizer and addition of ARC BBBE microbial agent, the expression of pyridoxine in the β-alanine metabolism pathway was upregulated in both spermidine and vitamin B6 pathways. In Fuhua 36 treated with bacterial agents, there was an upregulation in the expression of 10-formyl-THF within the carbon pool pathway, whereas the flavonoid pathway demonstrated a downregulation in the expression of red clover root glycoside. Similarly, the application of microbial agent to Liaohua 917 resulted in the downregulation of naringin expression in flavonoid metabolism and indole expression in benzoxazine metabolism.

Discussion

4-Aminobutyric acid (GABA) can be identified in seeds, rhizomes, and plant tissue fluids, such as those from beans and ginseng. The synthesis and conversion of GABA predominantly occur within the GABA pathway, including enzymes such as glutamate decarboxylase (GAD), γ-aminobutyric acid transaminase (GABA-T), and succinic semialdehyde dehydrogenase (SSADH). When plants encounter abiotic stresses such as salinity, drought, cold, or biotic stresses such as pathogen infection and insect feeding, they can rapidly accumulate GABA (Lin et al., 2014; Zhang et al., 2016). In our results, the downregulation of 4-aminobutyric acid expression under conventional fertilization conditions may indicate a decrease in disease or insect resistance in these two peanut varieties. We did not involve the mechanism of 4-aminobutyric acid here, and further research is needed.

Mannose, a monosaccharide structurally similar to glucose, is found in certain plant peels in a free state. However, it cannot be efficiently metabolized in the human body. It plays a role in immune system modulation and is involved in the capture of antigens by macrophage surface receptors that contain mannose components. Additionally, mannose contributes to wound healing acceleration, possesses anti-inflammatory properties, hinders tumor growth and metastasis, ultimately enhancing cancer survival rates, and prevents particular bacterial infections, such as urinary tract infections. Mannose is a distinctive attribute of peanut quality. In the context of conventional fertilization, the

http://www.aloki.hu ● ISSN 1589 1623 (Print) ● ISSN 1785 0037 (Online)
DOI: http://dx.doi.org/10.15666/aeer/2301_061078

downregulation of mannose expression suggests that these peanut varieties may not be suitable for direct consumption. However, as we do not have actual measured quantities, it is not clear whether the fertilizer application is the driving force of the mannose expression.

Indole acetic acid (IAA), a plant hormone, holds the distinction of being one of the earliest identified hormones present widely in nature. IAA plays a pivotal role in shaping gene expression among diverse microorganisms and serves as a signaling molecule mediating the intricate interplay between microorganisms and plants (Jameson, 2000; Fu et al.,2015). Sun (2014) demonstrated that IAA is the primary determinant governing interspecies competition among fungi coexisting in the same niche, as is evident in Cordyceps. Furthermore, exogenous auxin can promote susceptibility of host pathogens and facilitate the development of disease symptoms (Spaepen, 2011). The expression of indole-3-acetic acid (IAA) in the two varieties under the application of ARC BBBE microbial agent has not been extensively studied, which may be due to the different field growth trends of the two varieties caused by indole-3-acetic acid.

Author contributions. 1. Qiujun Lin: Conceptualization, Methodology, Software, Investigation, Formal Analysis, Writing-Original Draft. 2. Xiaofeng Yue: Original Draft, Resources. 3. Xianxin Wu: Data Curation, Writing - Original Draft, Writing - Review & Editing. 4. Chunjing Guo: Visualization, Investigation, Writing-Review & Editing. 5. Xun Zou: Resources, Investigation. 6. Li Guang: Resources, Investigation. 7. Jianzhong Wang (Corresponding Author): Conceptualization, Funding Acquisition, Resources, Supervision, Writing - Review & Editing.

Acknowledgements. We appreciate very much to the team of Academician Li Peiwu from the Oil Crop Research Institute of the Chinese Academy of Agricultural Sciences.

Funding. This study was supported by the Doctoral Initiation Project of the Dean's Fund of Liaoning Academy of Agricultural Sciences（2023BS0803）, the Opening Project of Key Laboratory of Detection for Mycotoxins, Ministry of Agriculture and Rural Affairs, China (SWDSJC2023002),the Fundamental Research Funds of Liaoning Academy of Agricultural Sciences（2023JCX0402）, Hubei Province Major Science and Technology Special Project (Key Application Technology Research on Quality Improvement and Nitrogen Fixation Coupling of Typical Grain and Oil Crops) (2023BBA002), Risk assessment of key technologies for controlling toxicity, fixing nitrogen, improving quality and increasing yield in peanuts and soybeans (GJFP20240101).

Conflict of interests. The authors declare that they have no competing interests.

Availability of data and materials. The datasets used and analyzed during this study are available from the corresponding author upon reasonable request.

REFERENCES

[1] Boulesteix, A., Strimmer, K. (2007): Partial least squares: a versatile tool for the analysis of high-dimensional genomic data. – Briefings in Bioinformatics 8: 32-44.

[2] Camargo, A. C. D., Canniatti-Brazaca, S. G. (2014): Peanuts as a Source of Protein, Unsaturated Fatty Acids, Tocopherol and Polyphenols. – In: Cook, R. W. (ed.) Peanuts: Production, Nutritional Content and Health Implications. Nova Publishers, New York.

[3] Chen, X., Xie, C., Sun, L. (2015): Longitudinal metabolomics profiling of Parkinson's disease-related α-synuclein A53T Transgenic Mice. – PloS ONE 10(8): e0136612.

[4] China Statistical Publishing House. (2022): China Statistical Yearbook. – China Statistical Publishing House, Beijing.

http://www.aloki.hu ● ISSN 1589 1623 (Print) ● ISSN 1785 0037 (Online)
DOI: http://dx.doi.org/10.15666/aeer/2301_061078

[5] Dunn, W. B., David, B., Paul, B. (2011): Procedures for large-scale metabolic profiling of serum and plasma using gas chromatography and liquid chromatography coupled to mass spectrometry. – Nature Protocols 6: 1060-1083.
[6] Frink, C. R., Waggoner, P. E., Ausubel, J. H. (1999): Nitrogen fertilizer: retrospect and prospect. – Proceedings of the National Academy of Sciences of the United States of America 96(4): 1175-1180.
[7] Fu, S. F., Wei, J. Y., Chen, H. W. (2015): Indole-3-acetic acid: a widespread physiological code in interactions of fungi with other organisms. – Plant Signal Behav. 10(8): e1048052.
[8] Jameson, P. (2000): Cytokinins and auxins in plant–pathogen interactions-an overview. – Plant Growth Regul 32: 369-80.
[9] Kanehisa, M. S. (2000): KEGG: Kyoto Encyclopedia of Genes and Genomes. – Nucleic Acids Research 28(1): 27-30.
[10] Lin, H., Rao, J., Shi, J. (2014): Seed metabolomic study reveals significant metabolite variations and correlations among different soybean cultivars. – Journal of Integrative Plant Biology 56(9): 826-836.
[11] Rao, J., Cheng, F., Hu, C. Y. (2014): Metabolic map of mature maize kernels. – Metabolomics 10: 775-787.
[12] Seifikalhor, M., Aliniaeifard, S., Hassani, B. (2019): Diverse role of γ-aminobutyric acid in dynamic plant cell responses. – Plant Cell Reports 38(8): 847-867.
[13] Shen, X. F., Lu, W. T., Chen, Y. A. (2022): Metabolomics method based on UPLC-MS/MS technology to study root metabolism of peanuts under aluminum stress. – Chinese Journal of Oil Crops 44(4): 833-844.
[14] Sithole, T. R., Ma, Y. X., Qin, Z. (2022): Influence of peanut varieties on the sensory quality of peanut butter. – Foods 11(21): 3499.
[15] Spaepen, S., Vanderleyden, J. (2011): Auxin and plant—microbe interactions. – Cold Spring Harb Perspect Biol 3: a001438.
[16] Sun, P. F., Fang, W. T., Shin, L. Y. (2014): Indole-3-acetic acid-producing yeasts in the phyllosphere of the carnivorous plant Drosera indica, L. – PLoS One 9: e114196.
[17] Sunita, A. R., Stephen, D. T., Matthew, G. (2017): γ-Aminobutyric acid (GABA) signalling in plants. – Cellular and Molecular Life Sciences 74: 1577-1603.
[18] Wang, J. B., Pu, S. B., Sun, Y. (2014): Metabolomic profiling of autoimmune hepatitis: the diagnostic utility of nuclear magnetic resonance spectroscopy. – Journal of Proteome Research 13(8): 3792-3801.
[19] Wei, D. H., Xie, D. C., Lu, M. L. (2017): Characterization of white tea metabolome: comparison against green and black tea by a nontargeted metabolomics approach. – Food Research International 96: 40-45.
[20] Wen, B., Mei, Z., Zeng, C. (2017): MetaX: a flexible and comprehensive software for processing metabolomics data. – BMC Bioinformatics 18(1): 183.
[21] Wilson, I. D., Gika, H., Theodoridis, G. (2010): Global metabolic profiling procedures for urine using UPLC-MS. – Nature Protocol 5(6): 1005-1018.
[22] Wu, Q., Li, C., Zhang, D. (2022): Nitrogen modified atmosphere packaging maintains the bioactive compounds and antioxidant capacity of postharvest fresh edible peanuts. – Postharvest Biology and Technology 190: 111957.
[23] Xie, C., Dang, X. S., Liu, N. (2021): Quality formation patterns of peanut varieties with different grain types. – Chinese Journal of Oil Crops 43(05): 795-802.
[24] Zhang, Y. F., Wang, H., Ding, Z. T. (2016): Mineral and metabolic profiles in tea leaves and flowers during flower development. – Plant Physiology and Biochemistry 106: 316-326.
[25] Zhao, J. X., Yin, X. Z., Xu, J. (2024): Analysis of quality characteristics of fried peanut kernels. – Journal of Peanut Science 53(3): 80-87.

http://www.aloki.hu ● ISSN 1589 1623 (Print) ● ISSN 1785 0037 (Online)
DOI: http://dx.doi.org/10.15666/aeer/2301_061078